A Study of the Development of the Stress Optic Law of Photoelastic Experiment Considering Residual Stress

Jae-guk Suh
Department of Automotive Management, Kyungdong College of Techno-Information, Gyungsan City, Kyungbuk 712-900, Korea
Jai-sug Hawong, Dong-chul Shin
School of Mechanical Engineering, Yeungnam University, Gyungsan City, Kyungbuk 712-749, Korea

Photoelastic experiment has two significant problems. The first problem is manufacturing a model specimen for complicated shapes of structures. The second problem is residual stress contained in the photoelastic model material. In this paper, the stress optic law that can be effecitvely used on photoelastic model materials with residual stress is developed. By using the stress optic law as developed in this research, we can obtain good results in photoelastic experiments using model material in which residual stress is contained. It is assured that the stress optic law developed in this research is useful. Therefore, it is suggested that the stress optic law considering residual stress can be applied to the photoelastic experiment for the stress analysis of the composite materials or bi-materials in which the residual stress is easily contained.

Key Words : Photoelasticity, Stress Optic Law, Residual Stress, Stress Distribution, Stress Concentration, Stress Intensity Factor

1. Introduction

Photoelastic experimental method has been used to stress analysis of structure or substructure and stress analysis in the vicinity of the crack tip (Smith and Smith, 1972; Etheridge and Dally, 1978; Sanford and Dally, 1979; Sanford, 1980; Hawong et al., 2002; Lee and Yin, 2002). Model experiments such as the photoelastic experiment have been restricted by two significant problems as follows. The first is the problem of modeling for the complicated body and the second is the problem of residual stress contained in photoelastic model materials. The residual stress in the photoelastic materials is produced by modeling, cutting and time effects, etc. Especially, large residual stress exists on the interface of the photoelastic model material of bi-material. Various kinds of residual stress exist in various photoelastic model materials. But small residual stress which occurs in the photoelastic model materials is usually neglected in the photoelastic experiments. The residual stress causes some errors in the results of photoelastic experiments.

In this paper, the stress optic law that can be used in photoelastic model materials with residual stress is developed. It is called the stress optic law considering residual stress. It is assured from Figs. 6, 7, 10 and Table 2 that the stress optic law considering residual stress developed in this paper is effective.

By using the stress optic law considering residual stress we can obtain good results in photoelastic experiments in which residual stress is contained. The stress optic law considering residual

* Corresponding Author,
E-mail : jshawong@yumail.ac.kr
TEL : +82-53-810-2445; **FAX** : +82-53-813-3703
School of Mechanical Engineering, Yeungnam University, Gyungsan City, Kyungbuk 712-749, Korea.
(Manuscript **Received** February 14, 2003; **Revised** August 22, 2003)

stress can be applied to obtain the good results in photoelastic experiments for the composite materials and bimaterials.

2. Development of Stress Optic Law Considering Residual Stress

2.1 General stress optic law

Equation (1) is a stress optic law for photoelastic experiment material without residual stress.

$$\frac{f \cdot N}{t}=\sigma_1-\sigma_2=\sqrt{(\sigma_x-\sigma_y)^2+4\tau^2_{xy}} \qquad (1)$$

where N is the fringe order ; f and t are stress fringe value and thickness of specimen respectively ; σ_1 and σ_2 are principal stresses.

2.2 Stress optic law considering residual stress

If there exists large residual stress or large residual fringe orders in the photoelastic experimental specimen, good experimental results can't be obtained from Eq. (1). It is very difficult to make the perfect photoelastic experiment models without residual stresses, especially in composite materials or bimaterials.

Equation (2) is the stress optic law for the relationship between residual stresses and residual fringe orders, that is in Fig. 1(a). Equation (3) and (4) are the stress optic law for a specimen with residual stress under loads of P_1 and P_2, respectively, in Fig. 1(b) and (c)

$$\left(\frac{f \cdot N_0}{t}\right)^2=(\sigma_{x0}-\sigma_{y0})^2+4\tau^2_{xy0} \qquad (2)$$

$$\left(\frac{f \cdot N_1}{t}\right)^2=\{(\sigma_{x1}+\sigma_{x0})-(\sigma_{y1}+\sigma_{y0})\}^2+4(\tau_{xy1}+\tau_{xy0})^2 \qquad (3)$$

$$\left(\frac{f \cdot N_2}{t}\right)^2=\{(m\sigma_{x1}+\sigma_{x0})-(m\sigma_{y1}+\sigma_{y0})\}^2+4(m\tau_{xy1}+\tau_{xy0})^2 \qquad (4)$$

where N_0=residual fringe orders, $N_1(N_2)$ =fringe orders at load $P_1(P_2)$, σ_{x0}, σ_{y0}, τ_{xy0} : residual stress components of the photoelastic experimental specimen, σ_{x1}, σ_{y1}, τ_{xy1} : stress components associated with P_1, R_1, Q_1 : external loads, P_2, R_2, Q_2 : other external loads, m : load ratio=(P_2/P_1) where direction of load, P_1 is identical to the direction of load P_2 but the magnitude of each load is different.

Substituting Eq. (2) for Eq. (3) and Eq. (4) respectively, and using the relationship of, "Eq. (4) −Eq. (3) ×m", Eq. (5) is obtained (Suh, 1995).

$$(\sigma_{x1}-\sigma_{y1})+4\tau_{xy1}=\frac{f^2 \cdot [N_2^2+(m-1)N_0^2-mN_1^2]}{m(m-1)t^2} \qquad (5)$$

We can see that residual stress components σ_{x0}, σ_{y0},, τ_{xy0} do not exist in the left and right sides of Eq. (5). Equation (5) is represented by fringe orders N_0, N_1, N_2 and load ratio m. Therefore, Eq. (5) is the stress optic law considering residual stress. The equation can be usefully applied to the

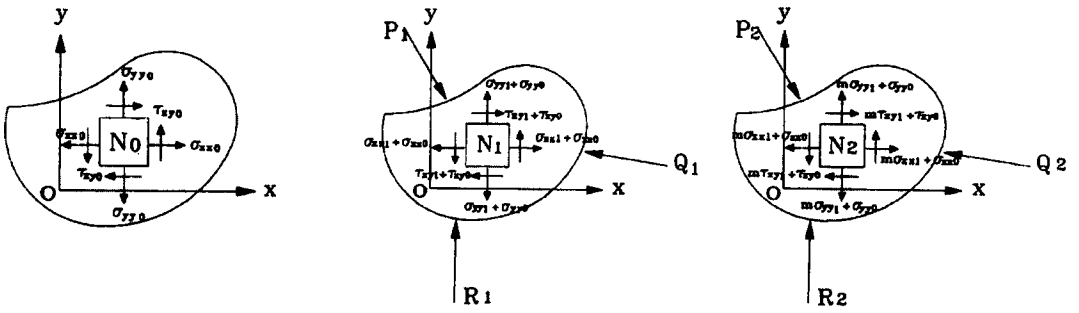

(a) Residual stress state

(b) Superposition of residual stress on the stress due to load P_1, R_1 and Q_1

(c) Superposition of residual stress on the stress due to load P_2, R_2 and Q_2

Fig. 1 Stress components in the body with residual stresses

photoelastic experimental specimen with residual stress.

2.3 Stress components of disk under diametral compression load

$$\sigma_{x1}=\frac{2P_1}{\pi t}\cdot\left(\frac{1}{d}-\frac{\cos\theta_1\sin^2\theta_1}{r_1}-\frac{\cos\theta_2\sin^2\theta_2}{r_2}\right)$$
$$\sigma_{y1}=\frac{2P_1}{\pi t}\cdot\left(\frac{1}{d}-\frac{\cos^3\theta_1}{r_1}-\frac{\cos^3\theta_2}{r_2}\right) \quad (6)$$
$$\tau_{xy1}=\frac{2P_1}{\pi t}\cdot\left(\frac{\cos^2\theta_1\sin\theta_1}{r_1}-\frac{\cos^2\theta_2\sin\theta_2}{r_2}\right)$$

Equation (6) represents the stress components in the arbitrary point q on the disk subjected to a diametral compressive load P_1 in the y-direction as shown in Fig. 2.

When loads of $P_1(=P)$ and P_0 are simultaneously applied to the disk as in Fig. 2, the stress components σ_x, σ_y, τ_{xy} in the point q on the disk are obtained from Eq. (7) by adding σ_{x1}, σ_{y1}, τ_{xy1} associated with P_1 to σ_{x0}, σ_{y0}, τ_{xy0} associated with P_0

$$\begin{aligned}\sigma_x&=\sigma_{x1}+\sigma_{x0}\\ \sigma_y&=\sigma_{y1}+\sigma_{y0}\\ \tau_{xy}&=\tau_{xy1}+\tau_{xy0}\end{aligned} \quad (7)$$

Equation (8) shows stress components of a point q in the disk when loads of P_2 and P_0 are simultaneously applied to the disk as shown in Fig. 2

$$\begin{aligned}\sigma_x&=m\sigma_{x1}+m\sigma_{x0}\\ \sigma_y&=m\sigma_{y1}+m\sigma_{y0}\\ \tau_{xy}&=m_{xy1}+m\tau_{xy0}\end{aligned} \quad (8)$$

where m is the load ratio P_2/P_1, and loads P_1 and P_2 have the same direction but different magnitudes.

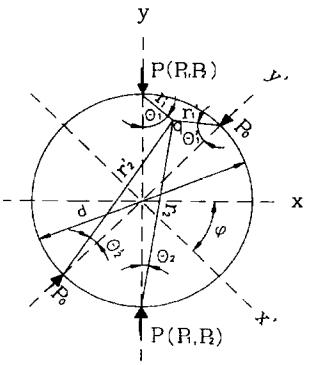

Fig. 2 Disk under diametral compressive load

3. Experiment and Discussion

The validity of stress optic law developed in this paper was studied by the following experiments: a disk under diametral compressive load and plates containing a hole or crack(model) under uniform tension.

3.1 Disk under diametral compression

Two disks are made from epoxy resin plate, their diameter and thickness are 50 mm and 6.45 mm, respectively. According to the stress freezing cycle of epoxy resin, stress freezing was done in the specimen under stress freezing load of P_0 (=10.78 N) as shown in Fig. 2.

Frozen stresses were used as residual stress. After stress freezing, diametral compressive loads P(=0, 529, 823, 1117 N) were applied to the specimen in the direction, as shown in Fig. 2. On the other hand, diametral compressive loads P (=627, 823, 901 N) were applied to the specimen without residual stresses.

Generally, the quantities of residual stress are unknown. But if we use these frozen stresses as residual stresses, we can get the quantities of residual stresses and plot graphic fringe patterns by using a computer. The validity of the stress optic law considering residual stress of Eq. (5) was verified by comparing experimental photoelastic fringe patterns with graphic fringe patterns plotted by the computer as follows.

Figure 3(a) shows photoelastic fringe patterns of the disk on which stress freezing is done at P_0 (=10.78 N). The frozen stresses may be regarded as residual stresses. Figures 3(b), (c) and (d) respectively show photoelastic fringe patterns in which fringe patterns of diametral compressive load P_1, associated with 529, 823 and 1117 N, are superposed upon those of residual stress shown in Fig. (3), Fig. (4) shows graphic isochromatic fringe patterns plotted by general stress optic law of Eq. (1), that is, they are graphic isochromatic fringe patterns of stress components of disk under P_0 and P_1.

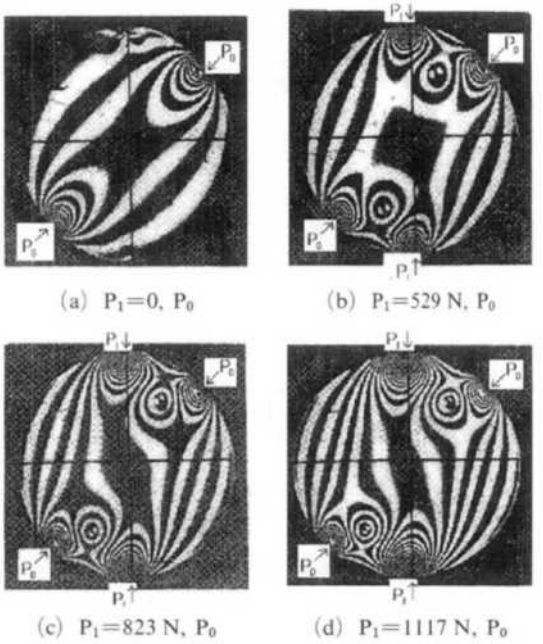

Fig. 3 Isochromatic fringe patterns of the disk under diametral compressive load (P_0: stress freezing load)

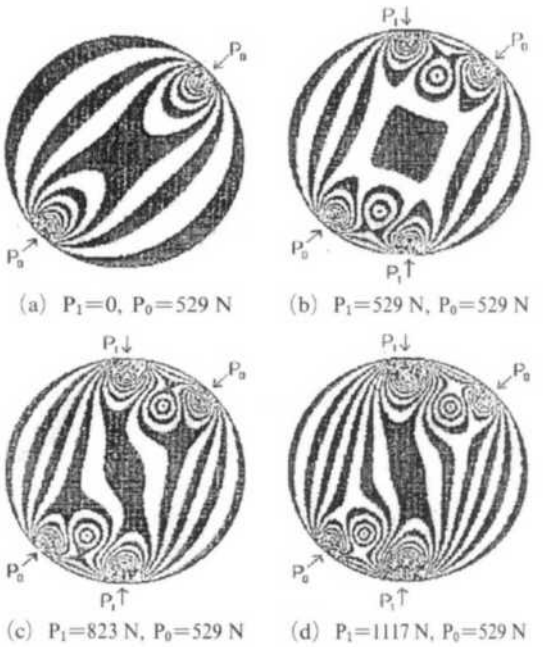

Fig. 4 Graphic fringe patterns of the disk with residual stresses and under diametral compressive loads

Figure 4(a) is the graphic isochromatic fringe patterns of a disk under diametral compressive load of $P_0(=529\ N)$. It was considered as the initial residual isochromatic fringe patterns of specimen. Figures 4(b), (c) and (d) respecitively show graphic isochromatic fringe patterns of the disk under loads of $P_0(=529\ N)$ and $P_1(529, 823, 1117\ N)$. If we compare Fig. 3 with Fig. 4 in the same boundary condition, we know that experimental isochromatic fringe patterns of Fig. 3 are almost identical to the graphic isochromatic fringe patterns of Fig. 4. Therefore, graphic isochromatic fringe patterns of Fig. 4(a) can be regarded as a residual isochromatic fringe pattern.

Figure 5(a) shows a graphic isochromatic fringe pattern plotted by the right side term of Eq. (5), that is, the stress optic law considering residual stress, where N_0, N_1 and N_2 are measured from Fig. 4(a), (b), (c), (d) and load ratio (m) is 1.375 ($P_1=823\ N$, $P_2=1117\ N$). When load P_1 is 823 N and residual stress does not exist, the graphic isochromatic fringe pattern plotted by the general stress optic law of Eq. (1) and Eq. (6) coincides with the graphic isochromatic fringe

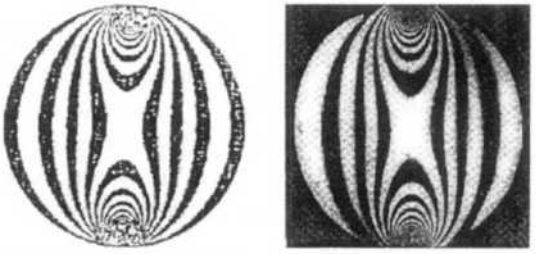

Fig. 5 Comparison of isochromatic fringe patterns

pattern of Fig. 5(a). Figure 5(a) also coincides with Fig. 5(b) which is an experimental fringe pattern of the disk without residual stress and under diametral compressive load of $P(=823\ N)$ in the y-direction. We know through these results that the stress optic law considering residual stress introduced in this paper is valid in the stress distribution and so is the isochromatic fringe graphic program developed in this research.

Figure 6 shows the non-dimensional values of $(\sigma_x-\sigma_y)\cdot dt/P$ of Eq. (6) with $2x/d$ where d is the circular diameter of the disk and x is x

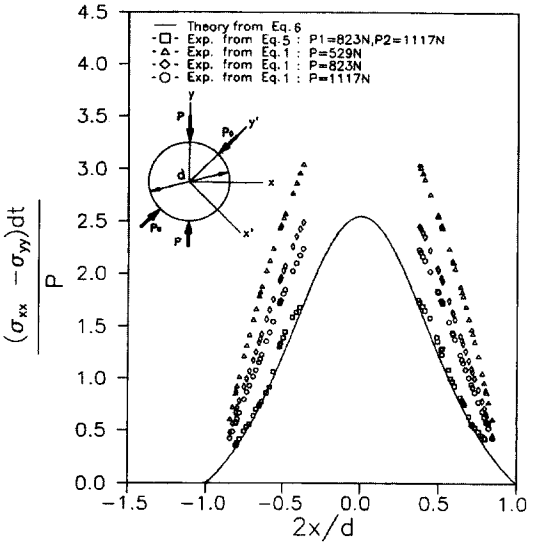

Fig. 6 Distributions of $(\sigma_x-\sigma_y)\cdot dt/P$ with $2x/d$ for actual isochromatic fringe patterns (Fig. 3) when residual stress exist

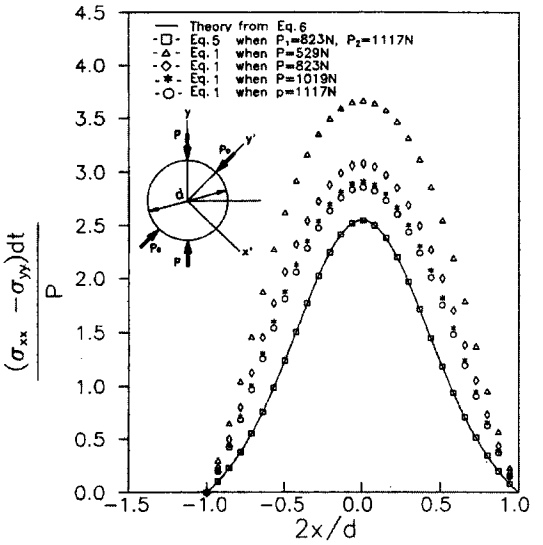

Fig. 7 Distributions of $(\sigma_x-\sigma_y)\cdot dt/P$ with $2x/d$ for graphic isochromatic fringe patterns (Fig. 4) when residual stress exist

coordinate. Square mark (-□-) is the result of Eq. (5), where N_0 is the fringe order in Fig. 3(a), N_1 in Fig. 3(c) and N_2 in Fig. 3(d). Errors between the result of Eq. (5) (-□-) and theoretical values(—) obtained from Eq. (6) equal 6 %. Triangle (-△-), diamond (-◇-) and circle mark (-○-) which respectively show the results of Eq. (1) in Fig. 3(b), (c) and (d) are much different from the theoretical result. We know from Fig. 6 that the larger the difference between the external load and initial load associated with residual stresses, the smaller the difference between the result of Eq. (1) and theoretical results. We can confirm the validity of Eq. (5) from Fig. 6.

The results of the graphic data of Fig. 4, under the same condition as the previous case, are shown in Fig. 7. The results (-□-) obtained from the stress optic law considering residual stress of Eq. (5) are perfectly identical to the theoretical results obtained from Eq. (6) in the graphic isochromatic fringe pattern. Triangle (-△-), diamond (-◇-) and circle mark (-○-) which show the results of Eq. (1) in Fig. 4(b), (c) and (d) are much different from the theoretical results (—) as shown in Fig. 6. Therefore, we know from Fig. 7 that the stress optic law considering residual stress developed in this research is useful on the graphic isochromatic fringe pattern with graphic residual fringe orders.

3.2 Plate containing a center hole under tensile load

Frozen stress was also used as residual stress in this experiment. Initial specimen size for stress freezing is 250 mm(x-axis direction) × 150 mm (y-axis direction) as shown in Fig. 8. This specimen has a center hole 10 mm in diameter. Stress freezing was done in this specimen by a frozen stress of σ_{02}(=52 kPa) as shown in Fig. 8. After stress freezing was done, the specimen was made so that the length of the y-axis is 30 mm and x-axis is 150 mm. The specimen also has a hole at the center. Tensile stresses σ_{01}(=0, 2.994, 4.448, 7.35 MPa) were applied to it in the direction of the x-axis as shown in Fig. 8.

Figure 9(a) shows the isochromatic fringe pattern of frozen stress. They were regarded as a residual isochromatic fringe pattern. Figures 9 (b), (c) and (d) respectively show isochromatic fringe patterns in which the photoelastic fringe pattern of tensile stress σ_{01}(=2.994, 4.448, 7.35 MPa) are superposed upon the residual photo-

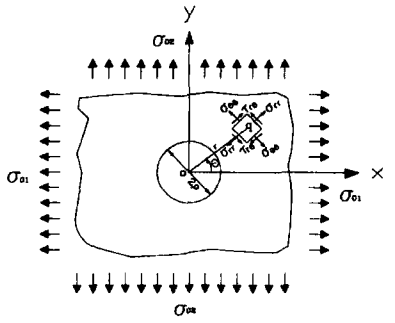

Fig. 8 Stress components around a hole of plate under tensile load

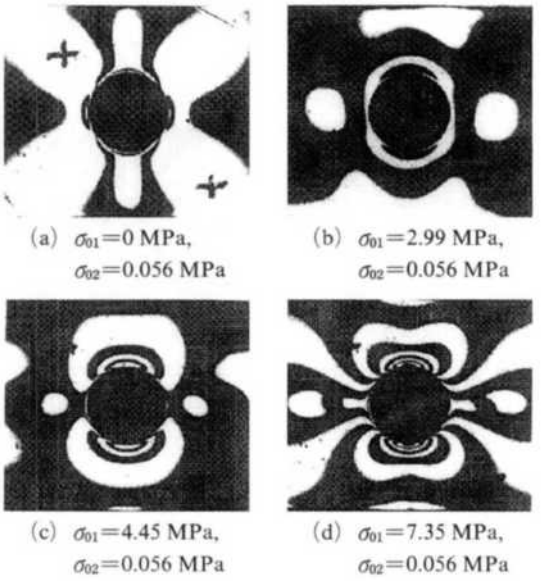

Fig. 9 Photoelastic fringe patterns of plates with a hole and with a residual stress ($=\sigma_{02}$) under tensile stress ($=\sigma_{01}$)

elastic fringe pattern of Fig. 9(a).

Figure 10 shows the distribution of non-dimensional stress ($\sigma_{\theta\theta}/\sigma_{01}$) around a hole obtained from Eq. (1), Eq. (5), and Howland's results (1930). Triangle marks (-△-) are the experimental results obtained from the isochromatic fringe pattern of Fig. 9(b) and the general stress optic law of Eq. (1). They are much different from Howland's results (—). By increasing external tension σ_{01}, they approach Howland's results. But they are also much different from Howland's results as shown in the star mark (-☆-) of Fig. 10. The results obtained from the stress optic law

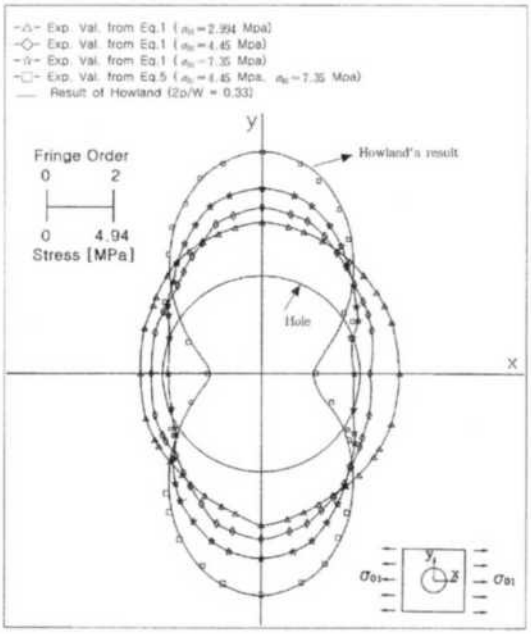

Fig. 10 Distribution of stress ($\sigma_{\theta\theta}/\sigma_{01}$) around the hole of the plate with residual stress

considering residual stress of Eq. (5) are almost equal to Howland's results where N_0's are fringe orders in Fig. 9(a), N_1 in Fig. 9(c) and N_2 in Fig. 9(d).

Therefore, we know that the stress optic law considering residual stress Eq. (5) developed in this research is also valid in the problems of stress concentration with a steep stress gradient.

3.3 Plate containing a center crack (Mode I)

Stresses generated during the molding process of the photoelastic experimental model material were used as residual stresses in this experiment. The specimen was molded by two times molding. A crack of the specimen was made by teflon sheet as follows.

First, half of the specimen (125 mm×31 mm) was made from epoxy plate which had already been molded to a thickness of 5.4 mm. Teflon sheet (width : 12.3 mm, thickness : 30 μm) was attached to the edge of the specimen (on the side of the width). This specimen was inserted into a molding box (width : 31 mm, length : 250 mm, thickness : 5.5mm).

Second, liquid from the epoxy resin was poured into the empty side of the molding box, and then a new specimen was molded according to the molding cycle of epoxy resin. After molding, the teflon sheet was pulled out from the new specimen. The space of the teflon sheet pulled out was almost equal to the natural crack. Many residual stresses sometimes exist in the bonded surface of the epoxy body. The experiment for mode I (2a/w=0.33) was done on the specimen containing residual stresses in the vicinity of the crack axis (bonded surface).

Figure 11 (a) shows the isochromatic fringe pattern of the state of residual stresses generated by two times molding. Figures 11 (b), (c) and (d) respectively show isochromatic fringe patterns which isochromatic fringe patterns associated with uniform tensions 1.437, 2.875, and 4.792 MPa normal to crack surface are superposed upon isochromatic fringe pattern of residual stress. Isochromatic fringe patterns of upper and lower parts in those figures are not symmetric because of residual stress.

Physical properties of first and second molding photoelastic model materials are shown in Table 1.

Because of being molded in the same condition, they are almost equal to each other. Table 2 shows stress intensity factors determined from the stress optic law considering residual stress Eq. (5) and the general stress optic law Eq. (1) in which the linear least squares method for photoelastic experiment (Sanford, 1980) is applied to the upper and lower parts of the isochromatic

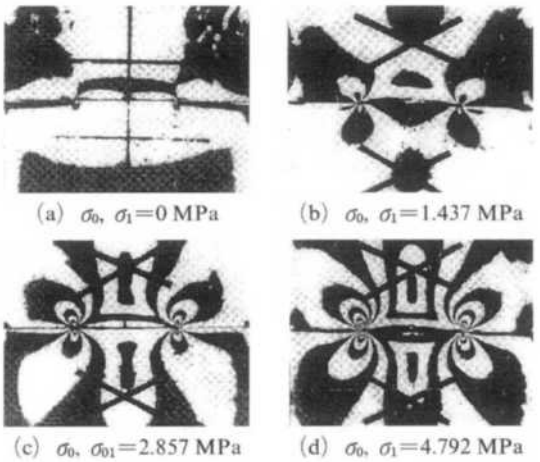

Fig. 11 Photoelastic fringe patterns in the vicinity of a crack tip under residual stress (σ_0) and tensile stresses (σ_1)

Table 1 Physical properties of the first molding material and the second molding material

Parts of specimen	Stress fringe value : f(kPa·m)	Young's modulus : E(MPa)	Poisson's ratio
The first molding (upper material)	11.66	3400	0.39
The second molding (lower material)	12.1	3342	0.40

Table 2 Stress intensity factor of specimen under mode I and with residual stress ($K_0=\sigma_0\sqrt{\pi a}$)

The parts of specimen			K_I/K_0	K_{II}/K_0
Exper. val. from Eq. (1)	upper part	P_0 : 235 N	0.982	0.173
		P_1 : 470 N	1.035	0.154
		P_2 : 784 N	1.095	0.102
	lower part	P_0 : 235 N	0.794	−0.242
		P_1 : 470 N	0.819	−0.228
		P_2 : 784 N	0.918	−0.193
Exper. val. from Eq. (5)	upper part		1.133	0.043
	lower part		1.151	0.010
Feddersen's results			1.112	0

fringe pattern shown in Fig. 11.

The results obtained from the general stress optic law Eq. (1) are different from Feddersen's results (1966) where load is mode I and $2a/w$ is 0.33. The value of K_{II}/K_0 is positive in the upper part and negative in the lower part. The value of K_I/K_0 is smaller than Fedderson's results by 20%. But all of the results of the lower and upper parts obtained from the stress optic law developed in this research are almost equal to Fedderson's results in K_I/K_0. Therefore, we can determine that the stress optic law considering residual stress developed in this research is valid in the analysis of the crack problem.

4. Conclusions

The following conclusions were obtained through experiments and discussions carried out in this article.

The stress optic law considering residual stress is developed. The validity is shown by the following photoelastic experiments: a disk under diametral compressive load, a plate containing a center hole under uniform tensile load, and a plate with a center crack under mode I etc.

Therefore, we know that the stress optic law considering residual stress is valid in the general stress analysis, the problems of stress concentration, and the problems of fracture mechanics, etc. Further, the stress optic law considering residual stress can be applied to the photoelastic experiment for the model materials with residual stress. It is expected that the stress optic law considering residual stress developed in this research may be usefully utilized in the photoelastic experimental model material for the bimaterials and composite materials.

Acknowledgment

This research was supported by the Yeungnam University research grants in 2003.

References

Etheridge, J. M. and Dally, J. W., 1978, "A Three Parameter Method for Determining Stress Intensity Factors from Isochromatic Fringe Loops," *Journal of Strain Analysis*, Vol. 13, No. 2, pp. 91~94.

Feddersen, C. E., 1966, "Discussion to: Plane strain crack Toughness Testing of high strength metallic materials," by William F. Brown, Jr., and John E. Strawley, *ASTM, Special Technical Publication*, No. 410, B. 77.

Hawong, Jai-Sug, Shin, Dong-Chul and Lee, Ouk-Sub, 2002, "A Study on the Initial Crack Curving Angle of Isotropic/Orthotropic Bimaterial," KSME International Journals, Vol. 16, No. 12, pp. 1594~1603.

Howland, R. L. T., 1930, "On the Stress in the Neighborhood of a Circular Hole in a Strip under Tension," *Phil. Trans. Roy. Soc.*, Vol. 229, pp. 48~86.

Lee, Ouk-Sub and Yin, Hai-Long, 2002, "Effect of Interface Hole Shape on Dynamic Interface Crack Propagation," Transactions of the KSME A, Vol. 26, No. 7, pp. 1217~1222.

Sanford, R. J. and Dally, J. W., 1979, "A General Method for Determining Mixed Mode Stress Intensity Factors from Isochromatic Fringe Patterns," *Engr. Fracture Mech.*, Vol. 11, No. 4, pp. 621~633.

Sanford, R. J., 1980, "Application of the Least Square Method to Photoelastic Analysis," *Experimental Mechanics*, Vol. 20, pp. 192~197.

Smith, D. G and Smith, C. W., 1972, "Photoelastic Determination of Mixed Stress Intensity Factors," *Engr. Fracture Mech.*, Vol. 4, pp. 357~366.

Suh, J. G., 1995, "A Study on the Development of Stress Optic Law Considering of Residual Stress in Photoelastic Experiment," PH. D. *Dissertation, Yeungnam University*, Kyungsan City, Korea.